Spin Squeezing with Short-Range Spin-Exchange Interactions

Michael A. Perlin,[1,2,*] Chunlei Qu,[3,†] and Ana Maria Rey[1,2]
[1]*JILA, National Institute of Standards and Technology and University of Colorado, 440 UCB, Boulder, Colorado 80309, USA*
[2]*Center for Theory of Quantum Matter, University of Colorado, Boulder, Colorado 80309, USA*
[3]*Department of Physics and Center for Quantum Science and Engineering, Stevens Institute of Technology, 1 Castle Point Terrace, Hoboken, New Jersey 07030, USA*

(Received 8 June 2020; revised 4 September 2020; accepted 7 October 2020; published 24 November 2020)

We investigate many-body spin squeezing dynamics in an XXZ model with interactions that fall off with distance r as $1/r^{\alpha}$ in $D = 2$ and 3 spatial dimensions. In stark contrast to the Ising model, we find a broad parameter regime where spin squeezing comparable to the infinite-range $\alpha = 0$ limit is achievable even when interactions are short ranged, $\alpha > D$. A region of "collective" behavior in which optimal squeezing grows with system size extends all the way to the $\alpha \to \infty$ limit of nearest-neighbor interactions. Our predictions, made using the discrete truncated Wigner approximation, are testable in a variety of experimental cold atomic, molecular, and optical platforms.

DOI: 10.1103/PhysRevLett.125.223401

Introduction.—Quantum technologies receive an enormous amount of attention for their potential to push beyond classical limits on physically achievable tasks. In order to be useful, however, these technologies must demonstrate a practical advantage over their classical counterparts. While most public attention has focused on a quantum advantage in the realm of computing, the quantum metrology community has made tremendous progress in developing strategies and platforms for surpassing classical limits on measurement precision [1–5]. A key element in these strategies is the use of entanglement to enhance the capabilities of individual, uncorrelated quantum systems. Spin squeezing is one of the most promising strategies for using entanglement to achieve a quantum advantage in practical sensing applications [6,7].

The paradigmatic setting for spin squeezing is the "one-axis twisting" (OAT) model [7,8], which generates spin-squeezed states by use of uniform infinite-range Ising interactions that do not distinguish between the constituent spins. These uniform interactions can be implemented directly via collisional interactions between delocalized atoms [9–11], as well as indirectly through coupling to collective phonon modes [12–14] or cavity photons [15–19]. Despite numerous proof-of-principle demonstrations, however, no spin squeezing experiment to date has achieved a practical metrological advantage, and current platforms relying on infinite-range interactions face a host of technical and fundamental difficulties that will require new breakthroughs to overcome.

The Ising model with power-law interactions that fall off with distance r as $1/r^{\alpha}$ generates squeezing that scales with system size when $\alpha < D$ in D spatial dimensions [20], which is highly desirable for metrological applications. Conversely, the power-law Ising model generates only a constant amount of squeezing that is independent of system size when $\alpha > D$. In practice, only a limited number of platforms can achieve long-range spin interactions ($\alpha < D$), making it highly desirable to shed light on the possibilities for scalable spin squeezing with short-range interactions ($\alpha > D$), which encompasses, e.g., superexchange, dipolar, van der Waals, and far-detuned phonon-mediated interactions.

Motivated by the intuition (echoed in Refs. [11,21–25]) that adding spin-exchange interactions to the Ising model should energetically protect collective behavior reminiscent of the OAT model, in this Letter we investigate the spin squeezing properties of the power-law XXZ model, whose ground-state physics was studied in Ref. [26]. Remarkably, we find a broad range of parameters for which the power-law XXZ model nearly saturates the amount of squeezing generated in the infinite-range ($\alpha = 0$) limit. Even when interactions are short ranged ($\alpha > D$), we observe a large region of collective squeezing behavior in which the amount of achievable spin squeezing grows with system size. This region extends through to the $\alpha \to \infty$ limit of nearest-neighbor interactions. Our Letter opens up a new prospect of spin squeezing in variety of cold atomic, molecular, and optical systems, including ultracold neutral atoms [27,28], Rydberg atoms [29,30], electric and magnetic dipolar quantum gases [31–34], and trapped ions [12,35].

Background and theory.—We begin with a brief review of spin squeezing and the OAT model, described by the Ising Hamiltonian

$$H_{\mathrm{OAT}} = \chi \sum_{i,j=1}^{N} s_{z,i} s_{z,j} = \chi S_z^2, \tag{1}$$

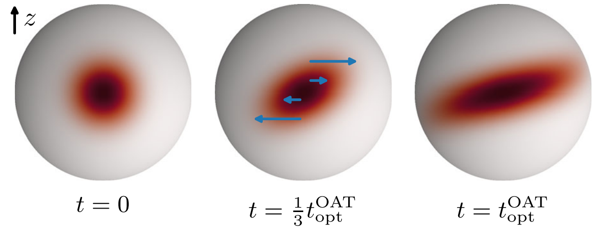

FIG. 1. Representations of the state $|\psi(t)\rangle$ of $N = 40$ spins initially polarized along the equator and evolved under the OAT Hamiltonian for a time t up to the optimal OAT squeezing time $\chi t_{\rm opt}^{\rm OAT} \sim 1/N^{2/3}$. Darker colors at a point $\hat{\boldsymbol{n}}$ on the sphere correspond to a larger overlap $|\langle \hat{\boldsymbol{n}}|\psi(t)\rangle|^2$, where $|\hat{\boldsymbol{n}}\rangle$ is a state in which all spins are polarized along $\hat{\boldsymbol{n}}$.

where χ is the OAT squeezing strength; the spin-z operator $s_{z,i} \equiv \sigma_{z,i}/2$ is defined in terms of the Pauli-z operator $\sigma_{z,i}$ on spin i; and $S_z \equiv \sum_{i=1}^{N} s_{z,i}$ is a collective spin-z operator. Eigenstates of $H_{\rm OAT}$ can be classified by a (non-negative) total spin $S \in \{N/2, N/2 - 1, \ldots\}$ and a projection $m_z \in \{S, S-1, \ldots, -S\}$ of spin onto the z axis. The manifold of all states with maximal total spin $S = N/2$ (e.g., spin-polarized states) is known as the "Dicke manifold" [7]. Equivalently, the Dicke manifold consists of all permutationally symmetric states that do not distinguish between underlying spins. States in the Dicke manifold can be represented by distributions on a sphere, whose variances along different axes must satisfy an appropriate set of quantum (Heisenberg) uncertainty relations (see Fig. 1). In the case of a single (two-level) spin, this distribution has a fixed Gaussian-like shape that is uniquely characterized by its orientation. Identifying the peak of this distribution recovers the representation of a qubit state by a point on the Bloch sphere. For $N > 1$ spins, meanwhile, this distribution can acquire additional structure with metrological utility.

Given an initial state of N spins polarized along the equator, represented by a Gaussian-like distribution on a sphere, the net effect of the OAT Hamiltonian is to shear this distribution, resulting in a *squeezed* state with a reduced variance $(\Delta\phi)^2$ along some axis. This reduced variance allows for an enhanced measurement sensitivity to rotations of the collective spin state along the squeezed axis, at the expense of a reduced sensitivity to rotations along an orthogonal axis. Spin squeezing can be quantified by the maximal gain in angular resolution $\Delta\phi$ over that achieved by a spin-polarized state [7],

$$\xi^2 \equiv \frac{(\Delta\phi_{\rm min})^2}{(\Delta\phi_{\rm polarized})^2} = \min_{\phi} {\rm var}(S_\phi^\perp) \times \frac{N}{|\langle \boldsymbol{S} \rangle|^2}, \qquad (2)$$

where $\boldsymbol{S} \equiv (S_x, S_y, S_z)$ is a vector of collective spin operators; the operator $S_\phi^\perp \equiv \boldsymbol{S} \cdot \hat{\boldsymbol{n}}_\phi^\perp$ is the projection of $\boldsymbol{S}$ onto an axis $\hat{\boldsymbol{n}}_\phi^\perp$ parametrized by an angle ϕ in the plane orthogonal to the mean spin vector $\langle \boldsymbol{S} \rangle$; and ${\rm var}(\mathcal{O}) \equiv \langle \mathcal{O}^2 \rangle - \langle \mathcal{O}^2 \rangle$ denotes the variance of $\mathcal{O}$. A spin squeezing parameter $\xi^2 < 1$ implies the presence of many-body entanglement [36] that enables a sensitivity to rotations beyond that set by classical limits on measurement precision [1]. The OAT model can prepare squeezed states with $\xi^2 \sim 1/N^{2/3}$, whereas the fundamental (Heisenberg) limit imposed by quantum mechanics is $\xi^2 \sim 1/N$ [1].

To accommodate for the fact that physical interactions are typically local, the OAT Hamiltonian in Eq. (1) can be modified by the introduction of coefficients $1/|\boldsymbol{r}_i - \boldsymbol{r}_j|^\alpha$ in the coupling between spins i and j at positions $\boldsymbol{r}_i$ and $\boldsymbol{r}_j$, resulting in the power-law Ising model. The introduction of nonuniform couplings means that the power-law Ising model breaks permutational symmetry, coupling the Dicke manifold of permutationally symmetric states with total spin $S = N/2$ to asymmetric states with $S < N/2$ and thereby invalidating the representation of squeezing dynamics shown in Fig. 1. The leakage of population outside the manifold of permutationally symmetric states can be energetically suppressed by the additional introduction of spin-aligning $\boldsymbol{s}_i \cdot \boldsymbol{s}_j$ interactions, where $\boldsymbol{s}_i \equiv (s_{x,i}, s_{y,i}, s_{z,i})$ is the spin vector for spin i. In total, we thus arrive at an XXZ model described by the Hamiltonian

$$H_{XXZ} = \sum_{i \neq j} \frac{J_\perp \boldsymbol{s}_i \cdot \boldsymbol{s}_j + (J_z - J_\perp) s_{z,i} s_{z,j}}{|\boldsymbol{r}_i - \boldsymbol{r}_j|^\alpha}. \qquad (3)$$

When interactions are uniform, $\alpha = 0$, the $\sum_{i \neq j} \boldsymbol{s}_i \cdot \boldsymbol{s}_j \sim \boldsymbol{S}^2 = S(S+1)$ term in Eq. (3) is a constant of motion within manifolds of definite total spin S, resulting in an OAT model with $\chi = J_z - J_\perp$.

When $J_z - J_\perp = 0$, the XXZ model contains only the spin-aligning $\boldsymbol{s}_i \cdot \boldsymbol{s}_j$ terms, and if interactions are long-ranged, $\alpha \leq D$, then the Dicke manifold is gapped away from all orthogonal states by a nonvanishing energy difference $\Delta_{\rm gap} \gtrsim |J_\perp|$ (see the Supplemental Material [37]). As a consequence, for any finite N and $\alpha \leq D$ there exists a nonvanishing range of coupling strengths $J_z \approx J_\perp$ for which a perturbative treatment of the anisotropic Ising terms in Eq. (3) is valid. In this case, the XXZ model becomes precisely the OAT model at first order in perturbation theory, with a squeezing strength $\chi_{\rm eff} = h_\alpha (J_z - J_\perp)$, where h_α is the average of $1/|\boldsymbol{r}_i - \boldsymbol{r}_j|^\alpha$ over all $i \neq j$. If interactions are short ranged with $\alpha > D$, then, generally, $\Delta_{\rm gap} \to 0$ as $N \to \infty$, formally invalidating perturbation theory for any J_z at sufficiently large N. Nonetheless, the spin-aligning terms of the XXZ model can still enable a nonperturbative emergence of collective behavior resembling perturbative gap-protected OAT. We numerically explore the prospect of spin squeezing with short-ranged interactions in the following section, finding that squeezing comparable to OAT may be possible with a wide range of α and J_z, including the $\alpha \to \infty$ limit of nearest-neighbor interactions.

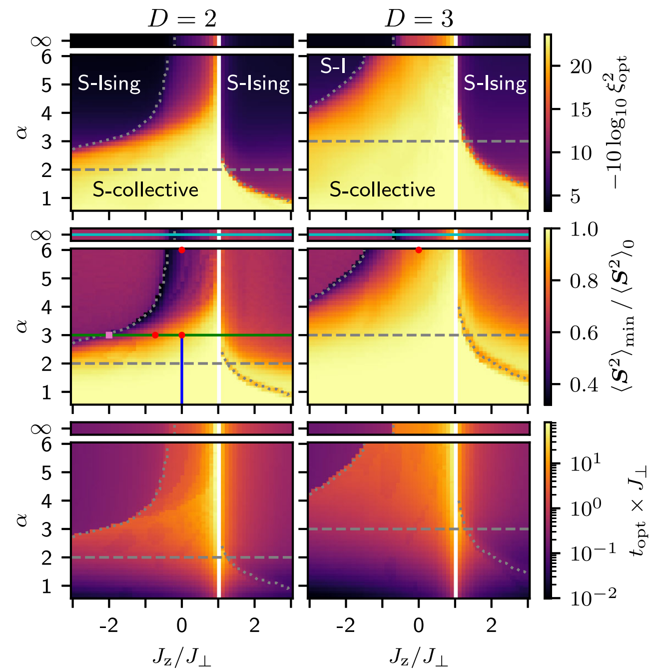

FIG. 2. The optimal squeezing $\xi^2_{\rm opt}$ (top), minimal squared magnetization $\langle \boldsymbol{S}^2\rangle_{\rm min}$ (middle), and optimal squeezing time $t_{\rm opt}$ (bottom) for $N = 4096 = 64^2 = 16^3$ spins in $D = 2$ (left) and $D = 3$ (right) spatial dimensions. Spins are initially polarized along the equator and evolved under the XXZ Hamiltonian in Eq. (3). Squeezing $\xi^2_{\rm opt}$ is shown in decibels, and $\langle \boldsymbol{S}^2\rangle_{\rm min}$ is normalized to its initial value $\langle \boldsymbol{S}^2\rangle_0 = (N/2)[(N/2)+1]$. Dashed gray lines mark $\alpha = D$, and dotted gray lines track local minima of $\langle \boldsymbol{S}^2\rangle_{\rm min}$, marking the boundary between regions of collective and Ising-limited squeezing dynamics, respectively, denoted "S-collective" and "S-Ising." Other markers in the middle panels indicate vales of $J_z/J_\perp, \alpha, D$ that are currently accessible with neutral atoms [42,43] (cyan line), Rydberg atoms [29,30,44] (red dots), polar molecules [31,32,45] (green line), magnetic atoms [33,34] (pink square), and trapped ions [12] (blue line). DTWA results are averaged over 500 trajectories.

Results.—Whereas the quantum Ising model is exactly solvable [38,39], the XXZ model in Eq. (3) is not. We therefore investigate the spin squeezing properties of the XXZ model using the discrete truncated Wigner approximation (DTWA) [40] for $N = 4096 = 64^2 = 16^3$ spins, focusing on the case of two ($D = 2$) and three ($D = 3$) spatial dimensions (see the Supplemental Material [37] for $D = 1$, where our main results are less striking but still hold). DTWA has been shown to accurately capture the behavior of collective spin observables in a variety of settings [40,41], and we provide additional benchmarking of DTWA for the XXZ model on lattices of up to 7×7 spins in the Supplemental Material [37], although it will ultimately be up to experiments to verify our findings. Our main results are summarized in Fig. 2, in which we explore the squeezing behavior of the XXZ model in Eq. (3) around the isotropic (Heisenberg) point at $J_z = J_\perp$ by varying both $J_z/J_\perp$ and the power-law exponent α. Specifically, we examine (i) the optimal squeezing parameter $\xi^2_{\rm opt} \equiv \min_t \xi^2(t) = \xi^2(t_{\rm opt})$, (ii) the minimal squared magnetization throughout squeezing dynamics, $\langle \boldsymbol{S}^2\rangle_{\rm min} \equiv \min_{t\le t_{\rm opt}} \langle \boldsymbol{S}^2\rangle(t)$, and (iii) the optimal squeezing time $t_{\rm opt}$.

First and foremost, Fig. 2 confirms the theoretical argument that OAT-limited squeezing should be achievable with any power-law exponent $\alpha \le D$ for some nonvanishing range of Ising couplings, $J_z \approx J_\perp$. Moreover, when $\alpha \le D$ we observe that this capability persists well beyond the perturbative window with $|J_z - J_\perp| \ll |J_\perp|$, covering all $J_z/J_\perp < 1$ shown in Fig. 2 and an increasing range of $J_z/J_\perp > 1$ as $\alpha \to 0$. Even more striking than the behavior at $\alpha \le D$, Fig. 2 shows that squeezing well beyond the Ising limit can still be achievable for a wide range of Ising couplings $J_z/J_\perp < 1$ when interactions are short ranged, $\alpha > D$. In a nearest-neighbor XXZ model ($\alpha \to \infty$), the region $|J_z| < |J_\perp|$ corresponds to the equilibrium XY phase, whereas $J_z/J_\perp < -1$ and $J_z/J_\perp > +1$ correspond to the equilibrium Ising ferromagnet and antiferromagnet phases (depending on the sign of $J_\perp$) [26,46]. The asymmetry about $J_z = J_\perp$ in Fig. 2 thus hints at an interesting connection between equilibrium physics [26] and far-from-equilibrium dynamical behavior of the XXZ model (discussed further in the next section) [47].

Though the attainable amount of squeezing generally decreases with shorter range (increasing α) and stronger anisotropy (decreasing $J_z/J_\perp < 1$), a region of collective squeezing behavior connected to the OAT limit persists through to the $\alpha \to \infty$ limit of nearest-neighbor interactions. This region is reminiscent of the $\frac{2}{3}D \le \alpha < D$ region of the power-law Ising model ($J_\perp = 0$), in which squeezing falls short of the OAT limit, but still grows with system size [20].

In fact, the transition between collective and Ising-limited squeezing regions, which we, respectively, denote S-collective and S-Ising (with an "S-" prefix to emphasize the role of squeezing in their characterization), is marked by a discontinuous change in both the minimal squared magnetization $\langle \boldsymbol{S}^2\rangle_{\rm min}$ and the optimal squeezing time $t_{\rm opt}$, signifying the presence of a dynamical phase transition. The dynamical phases in question can be characterized by the behavior of optimal squeezing $\xi^2_{\rm opt}$, which either scales with system size or saturates to a constant value. We discuss and clarify these points below.

The discontinuity in optimal squeezing time $t_{\rm opt}$ at the dynamical phase boundary in Fig. 2 is the result of a competition between local optima in squeezing over time, shown in Fig. 3. Large amounts of spin squeezing are generated in the S-collective phase near the isotropic point at $J_z = J_\perp$. The amount of squeezing generated by collective dynamics falls off away from the isotropic point, until it finally drops below an "Ising" squeezing peak that is generated at much short times, resulting in a discontinuous change in the time at which squeezing is optimal. The discontinuous change in the optimal squeezing time is, in

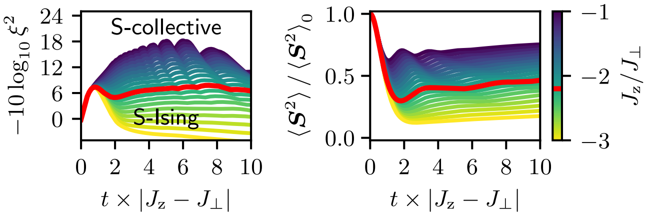

FIG. 3. Squeezing ξ^2 and squared magnetization $\langle \boldsymbol{S}^2 \rangle$ over time for the power-law XXZ model with $\alpha = 3$ on a 2D lattice of 64×64 spins. Color indicates the value of $J_z/J_\perp$, and red lines (at $J_z/J_\perp = -2.2$) mark the approximate transition between S-collective and S-Ising phases, when the collective squeezing peak at $\tau \equiv t \times |J_z - J_\perp| \sim 6$ drops below the Ising peak at $\tau \sim 1$. For the parameters shown, $\langle \boldsymbol{S}^2 \rangle$ reaches a minimum at $\tau \sim 2$, which means that optimal squeezing at $\tau \sim 1$ is reached before maximal decay of $\langle \boldsymbol{S}^2 \rangle$ in the S-Ising phase.

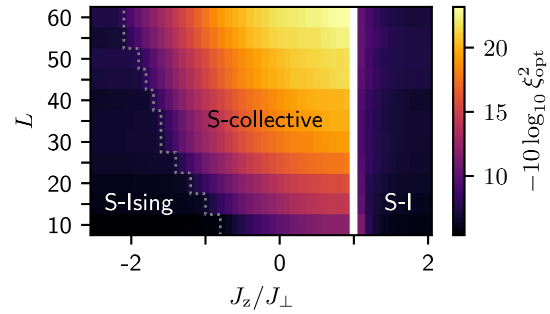

FIG. 4. Optimal squeezing ξ^2_{opt} as a function of system size for the power-law XXZ model with $\alpha = 3$ on a 2D lattice of $N = L \times L$ spins. Whereas the amount of squeezing generated in the S-Ising phase is insensitive to system size, squeezing in the S-collective phase grows with system size and as $J_z/J_\perp \to 1$ (from below). Dotted gray line tracks minima of $\langle \boldsymbol{S}^2 \rangle_{\mathrm{min}}$ as a function of $J_z/J_\perp$, as in Fig. 2, marking the approximate dynamical phase boundary.

turn, responsible for the sudden change in the minimal squared magnetization $\langle \boldsymbol{S}^2 \rangle_{\mathrm{min}}$, which has less time to decay in the Ising-limited (S-Ising) regime.

It is no surprise that quantities such as t_{opt} and $\langle \boldsymbol{S}^2 \rangle_{\mathrm{min}}$ that are defined via minimization exhibit discontinuous behavior, and these discontinuities do not by themselves indicate a transition between different phases of matter. We can formally distinguish the S-collective and S-Ising phases by examining the nature of squeezing that is generated in these regions. Specifically, the S-Ising phase generates an amount of squeezing that is insensitive to system size, whereas the S-collective phase generates an amount of squeezing that scales with system size as $\xi^2_{\mathrm{opt}} \sim 1/N^\nu$, where the exponent ν generally depends on the values of α and $J_z/J_\perp$ [37]. Numerically, we find that the S-collective phase spans all $J_z/J_\perp < 1$ when $\alpha \lesssim D$, whereas the transition between S-collective and S-Ising phases occurs at a critical Ising coupling J_z^{crit} that either diverges logarithmically with system size ($J_z^{\mathrm{crit}} \sim -\log N$) or stays constant when $\alpha \gtrsim D$ (see Fig. 4, where we focus on $D = 2$ and $\alpha = 3$ due to its experimental relevance, and the Supplemental Material [37]). We note that small oscillations in squeezing over time (see Fig. 3) add minor corrections to the behavior of ξ^2_{opt} and J_z^{crit}. These oscillations are responsible for the discontinuous behavior of t_{opt} and $\langle \boldsymbol{S}^2 \rangle_{\mathrm{min}}$ seen in Fig. 2 within the S-collective phase.

Discussion.—The mechanism behind the collective dynamics featured by the XXZ model far from the isotropic point at $J_z = J_\perp$ is not obvious and lies in a parameter regime beyond the reach of exact treatment with current theoretical capabilities. While an in-depth understanding of collective dynamics will most likely require experimental investigations in the spirit of quantum simulation, we discuss possible phenomenological explanations below.

Collective squeezing behavior when $\alpha < D$ is the least surprising, as the XXZ model essentially interpolates between perturbative gap-protected OAT (near $J_z = J_\perp$) and the long-range power-law Ising model (at $J_z \to \pm\infty$), both of which generate collective spin squeezing. When $\alpha > D$, as long as $D > 2$ or $\alpha < 2D$ (i.e., all $\alpha > 3$ when $D = 3$, and $2 < \alpha < 4$ when $D = 2$), a generalized version of the Mermin-Wagner theorem [48] allows for the existence of long-range order in the thermodynamic limit, below a critical temperature [23,24]. Our observations may therefore be indicative of thermalization to a long-range-ordered steady state in an equilibrium XY phase [47], with significant amounts of collective spin squeezing present in the transient dynamics. This explanation is supported by the fact that the squared magnetization $\langle \boldsymbol{S}^2 \rangle$ approaches a nonvanishing steady-state value in Fig. 3 (see also the Supplemental Material [37]). Nevertheless, the persistence of long-range order is a necessary but insufficient condition to characterize the types of dynamical phases considered in this Letter. Instead, these phases are defined operationally by whether attainable spin squeezing scales with system size and are thus sensitive to transient effects.

For even shorter-range interactions ($\alpha \geq 2D$) when $D \leq 2$, long-range order is forbidden in the steady state. Even so, a spin-polarized initial state can still take an appreciable amount of time to thermalize to a disordered steady state. Squeezing beyond the Ising limit can therefore occur as a transient phenomenon, before long-range order is disrupted [37].

Experimental applications.—As indicated in Fig. 2, our results are readily applicable to the generation of spin-squeezed states in a variety of experimental platforms that have been shown to implement the power-law XXZ model, including neutral atoms ($\alpha \to \infty$) [42,43], Rydberg atoms ($\alpha = 3$, 6) [29,30,44], polar molecules ($\alpha = 3$) [31,32,45], and magnetic atoms ($\alpha = 3$) [33,34]. Note that one may additionally have to consider the effects of a subunit filling fraction on the realization of a spin model. In principle, subunit filling introduces effective disorder into the XXZ spin couplings [24,49]. Nonetheless, the precise form of these interactions is not essential to the existence of an S-collective phase in the XXZ model, as evidenced by the fact that this phase persists through to the $\alpha \to \infty$ limit of nearest-neighbor interactions (see the Supplemental Material [37]).

Finally, we discuss the application of our results to Ising systems without 3D spin-aligning $\boldsymbol{s}_i \cdot \boldsymbol{s}_j$ interactions, as in the case of some Rydberg atom ($\alpha = 3$, 6) [29,30] and trapped ion ($0 \leq \alpha < 3$) [12] experiments. In this case, 2D spin-aligning interactions within the $y - z$ plane can still be engineered by the application of a strong transverse driving field ΩS_x. If the drive strength $|\Omega| \gg \frac{1}{2} N h_\alpha |J_z|$, with h_α the mean of $1/|\boldsymbol{r}_i - \boldsymbol{r}_j|^\alpha$ over all $i \neq j$, then moving into the rotating frame of the drive and eliminating fast-oscillating terms results in an XX model described by the Hamiltonian

$$H_{XX} = \frac{J_z}{2} \sum_{i \neq j} \frac{s_{y,i} s_{y,j} + s_{z,i} s_{z,j}}{|\boldsymbol{r}_i - \boldsymbol{r}_j|^\alpha}, \tag{4}$$

which is a special case of the XXZ model in Eq. (3), with $(J_\perp, J_z) \to (J_z/2, 0)$. Ising systems with a strong transverse field can thus access a vertical cut along $J_z/J_\perp = 0$ in Fig. 2. In a similar fashion, dynamic Hamiltonian engineering protocols [50,51] can transform the Ising model into an XXZ model with any $J_z/J_\perp \geq 0$, albeit at the cost of added complexity.

We thank Andrew Lucas, Thomas Bilitewski, Sean R. Muleady, and Jeremy T. Young for helpful technical discussions. This work is supported by the DARPA DRINQs grant, the ARO single investigator Grant No. W911NF-19-1-0210, NSF Grant No. PHY-1820885, AFOSR Grant No. FA9550-19-1-0275, NSF Grant No. PHY-1734006 (JILA-PFC), and by NIST.

[*] mika.perlin@gmail.com
[†] M. A. P. and C. Q. contributed equally to this work.

[1] V. Giovannetti, S. Lloyd, and L. Maccone, Quantum Metrology, Phys. Rev. Lett. **96**, 010401 (2006).
[2] V. Giovannetti, S. Lloyd, and L. Maccone, Advances in quantum metrology, Nat. Photonics **5**, 222 (2011).
[3] G. Tóth and I. Apellaniz, Quantum metrology from a quantum information science perspective, J. Phys. A **47**, 424006 (2014).
[4] M. Szczykulska, T. Baumgratz, and A. Datta, Multi-parameter quantum metrology, Adv. Phys. X **1**, 621 (2016).
[5] L. Pezzè, A. Smerzi, M. K. Oberthaler, R. Schmied, and P. Treutlein, Quantum metrology with nonclassical states of atomic ensembles, Rev. Mod. Phys. **90**, 035005 (2018).
[6] D. J. Wineland, J. J. Bollinger, W. M. Itano, F. L. Moore, and D. J. Heinzen, Spin squeezing and reduced quantum noise in spectroscopy, Phys. Rev. A **46**, R6797(R) (1992).
[7] J. Ma, X. Wang, C. P. Sun, and F. Nori, Quantum spin squeezing, Phys. Rep. **509**, 89 (2011).
[8] M. Kitagawa and M. Ueda, Squeezed spin states, Phys. Rev. A **47**, 5138 (1993).
[9] T. Zibold, E. Nicklas, C. Gross, and M. K. Oberthaler, Classical Bifurcation at the Transition from Rabi to Josephson Dynamics, Phys. Rev. Lett. **105**, 204101 (2010).
[10] M. J. Martin, M. Bishof, M. D. Swallows, X. Zhang, C. Benko, J. von-Stecher, A. V. Gorshkov, A. M. Rey, and J. Ye, A quantum many-body spin system in an optical lattice clock, Science **341**, 632 (2013).
[11] P. He, M. A. Perlin, S. R. Muleady, R. J. Lewis-Swan, R. B. Hutson, J. Ye, and A. M. Rey, Engineering spin squeezing in a 3D optical lattice with interacting spin-orbit-coupled fermions, Phys. Rev. Research **1**, 033075 (2019).
[12] J. W. Britton, B. C. Sawyer, A. C. Keith, C.-C. J. Wang, J. K. Freericks, H. Uys, M. J. Biercuk, and J. J. Bollinger, Engineered two-dimensional Ising interactions in a trapped-ion quantum simulator with hundreds of spins, Nature (London) **484**, 489 (2012).
[13] J. G. Bohnet, B. C. Sawyer, J. W. Britton, M. L. Wall, A. M. Rey, M. Foss-Feig, and J. J. Bollinger, Quantum spin dynamics and entanglement generation with hundreds of trapped ions, Science **352**, 1297 (2016).
[14] M. Gabbrielli, L. Lepori, and L. Pezzè, Multipartite-entanglement tomography of a quantum simulator, New J. Phys. **21**, 033039 (2019).
[15] K. Baumann, C. Guerlin, F. Brennecke, and T. Esslinger, Dicke quantum phase transition with a superfluid gas in an optical cavity, Nature (London) **464**, 1301 (2010).
[16] H. Ritsch, P. Domokos, F. Brennecke, and T. Esslinger, Cold atoms in cavity-generated dynamical optical potentials, Rev. Mod. Phys. **85**, 553 (2013).
[17] M. A. Norcia, R. J. Lewis-Swan, J. R. K. Cline, B. Zhu, A. M. Rey, and J. K. Thompson, Cavity-mediated collective spin-exchange interactions in a strontium superradiant laser, Science **361**, 259 (2018).
[18] R. M. Kroeze, Y. Guo, V. D. Vaidya, J. Keeling, and B. L. Lev, Spinor Self-Ordering of a Quantum Gas in a Cavity, Phys. Rev. Lett. **121**, 163601 (2018).
[19] E. J. Davis, G. Bentsen, L. Homeier, T. Li, and M. H. Schleier-Smith, Photon-Mediated Spin-Exchange Dynamics of Spin-1 Atoms, Phys. Rev. Lett. **122**, 010405 (2019).
[20] M. Foss-Feig, Z.-X. Gong, A. V. Gorshkov, and C. W. Clark, Entanglement and spin-squeezing without infinite-range interactions, arXiv:1612.07805.
[21] A. M. Rey, L. Jiang, M. Fleischhauer, E. Demler, and M. D. Lukin, Many-body protected entanglement generation in interacting spin systems, Phys. Rev. A **77**, 052305 (2008).
[22] P. Cappellaro and M. D. Lukin, Quantum correlation in disordered spin systems: Applications to magnetic sensing, Phys. Rev. A **80**, 032311 (2009).
[23] M. P. Kwasigroch and N. R. Cooper, Bose-Einstein condensation and many-body localization of rotational excitations of polar molecules following a microwave pulse, Phys. Rev. A **90**, 021605(R) (2014).
[24] M. P. Kwasigroch and N. R. Cooper, Synchronization transition in dipole-coupled two-level systems with positional disorder, Phys. Rev. A **96**, 053610 (2017).
[25] E. J. Davis, A. Periwal, E. S. Cooper, G. Bentsen, S. J. Evered, K. Van Kirk, and M. H. Schleier-Smith, Protecting Spin Coherence in a Tunable Heisenberg Model, Phys. Rev. Lett. **125**, 060402 (2020).

[26] I. Frérot, P. Naldesi, and T. Roscilde, Entanglement and fluctuations in the *XXZ* model with power-law interactions, Phys. Rev. B **95**, 245111 (2017).

[27] M. A. Cazalilla and A. M. Rey, Ultracold fermi gases with emergent SU(n) symmetry, Rep. Prog. Phys. **77**, 124401 (2014).

[28] C. Gross and I. Bloch, Quantum simulations with ultracold atoms in optical lattices, Science **357**, 995 (2017).

[29] C. S. Adams, J. D. Pritchard, and J. P. Shaffer, Rydberg atom quantum technologies, J. Phys. B **53**, 012002 (2019).

[30] A. Browaeys and T. Lahaye, Many-body physics with individually controlled Rydberg atoms, Nat. Phys. **16**, 132 (2020).

[31] J. L. Bohn, A. M. Rey, and J. Ye, Cold molecules: Progress in quantum engineering of chemistry and quantum matter, Science **357**, 1002 (2017).

[32] S. A. Moses, J. P. Covey, M. T. Miecnikowski, D. S. Jin, and J. Ye, New frontiers for quantum gases of polar molecules, Nat. Phys. **13**, 13 (2017).

[33] S. Lepoutre, J. Schachenmayer, L. Gabardos, B. Zhu, B. Naylor, E. Maréchal, O. Gorceix, A. M. Rey, L. Vernac, and B. Laburthe-Tolra, Out-of-equilibrium quantum magnetism and thermalization in a spin-3 many-body dipolar lattice system, Nat. Commun. **10**, 1714 (2019).

[34] A. Patscheider, B. Zhu, L. Chomaz, D. Petter, S. Baier, A.-M. Rey, F. Ferlaino, and M. J. Mark, Controlling dipolar exchange interactions in a dense three-dimensional array of large-spin fermions, Phys. Rev. Research **2**, 023050 (2020).

[35] C. D. Bruzewicz, J. Chiaverini, R. McConnell, and J. M. Sage, Trapped-ion quantum computing: Progress and challenges, Appl. Phys. Rev. **6**, 021314 (2019).

[36] A. S. Sørensen and K. Mølmer, Entanglement and Extreme Spin Squeezing, Phys. Rev. Lett. **86**, 4431 (2001).

[37] See Supplemental Material at http://link.aps.org/supplemental/10.1103/PhysRevLett.125.223401 for auxiliary numerical benchmarking and more detailed analyses of quantum dynamics.

[38] M. Foss-Feig, K. R. A. Hazzard, J. J. Bollinger, and A. M. Rey, Nonequilibrium dynamics of arbitrary-range Ising models with decoherence: An exact analytic solution, Phys. Rev. A **87**, 042101 (2013).

[39] M. van den Worm, B. C. Sawyer, J. J. Bollinger, and M. Kastner, Relaxation timescales and decay of correlations in a long-range interacting quantum simulator, New J. Phys. **15**, 083007 (2013).

[40] J. Schachenmayer, A. Pikovski, and A. M. Rey, Many-Body Quantum Spin Dynamics with Monte Carlo Trajectories on a Discrete Phase Space, Phys. Rev. X **5**, 011022 (2015).

[41] J. Schachenmayer, A. Pikovski, and A. M. Rey, Dynamics of correlations in two-dimensional quantum spin models with long-range interactions: A phase-space Monte-Carlo study, New J. Phys. **17**, 065009 (2015).

[42] L.-M. Duan, E. Demler, and M. D. Lukin, Controlling Spin Exchange Interactions of Ultracold Atoms in Optical Lattices, Phys. Rev. Lett. **91**, 090402 (2003).

[43] Y.-A. Chen, S. Nascimbène, M. Aidelsburger, M. Atala, S. Trotzky, and I. Bloch, Controlling Correlated Tunneling and Superexchange Interactions with ac-Driven Optical Lattices, Phys. Rev. Lett. **107**, 210405 (2011).

[44] A. Signoles, T. Franz, R. F. Alves, M. Gärttner, S. Whitlock, G. Zürn, and M. Weidemüller, Glassy dynamics in a disordered Heisenberg quantum spin system, arXiv:1909.11959.

[45] A. V. Gorshkov, S. R. Manmana, G. Chen, J. Ye, E. Demler, M. D. Lukin, and A. M. Rey, Tunable Superfluidity and Quantum Magnetism with Ultracold Polar Molecules, Phys. Rev. Lett. **107**, 115301 (2011).

[46] *Quantum Magnetism*, edited by U. Schollwöck, J. Richter, D. J. J. Farnell, and R. F. Bishop, Lecture Notes in Physics Vol. 645 (Springer, Berlin, 2004).

[47] In fact, when $J_\perp < 0$ the S-collective region at $J_z/J_\perp < 1$ is contained *within* the ground-state *XY* phase of the power-law *XXZ* model [26].

[48] P. Bruno, Absence of Spontaneous Magnetic Order at Nonzero Temperature in One- and Two-Dimensional Heisenberg and *XY* Systems with Long-Range Interactions, Phys. Rev. Lett. **87**, 137203 (2001).

[49] K. R. A. Hazzard, S. R. Manmana, M. Foss-Feig, and A. M. Rey, Far-from-Equilibrium Quantum Magnetism with Ultracold Polar Molecules, Phys. Rev. Lett. **110**, 075301 (2013).

[50] J. Choi, H. Zhou, H. S. Knowles, R. Landig, S. Choi, and M. D. Lukin, Robust Dynamic Hamiltonian Engineering of Many-Body Spin Systems, Phys. Rev. X **10**, 031002 (2020).

[51] H. Zhou, J. Choi, S. Choi, R. Landig, A. M. Douglas, J. Isoya, F. Jelezko, S. Onoda, H. Sumiya, P. Cappellaro, H. S. Knowles, H. Park, and M. D. Lukin, Quantum Metrology with Strongly Interacting Spin Systems, Phys. Rev. X **10**, 031003 (2020).